

Wide Band L-Probe Fed Circular Patch Antenna with Elliptical Parasitic Patch and Two Elements Array

Muhammad N. Islam^{1, 2, *}, Markus Berg², Timo Tarvainen¹, and Erkki T. Salonen²

Abstract—To enable the quest for high data rates in telecommunications, wide-band radio designs as well as antennas are required. This paper demonstrates a unique bandwidth enhancement technique for L-probe fed patch antenna. This is a novel technique to enhance patch antenna bandwidth with desired radiation properties. One circular shape main patch and two elliptical shape parasitic patches on PCB give wide-band response by exciting multiple resonances. The designed antenna array gives almost 45%, –10 dB impedance matched relative bandwidth. This is a very simple and inexpensive patch antenna solution for the wide-band wireless application. A two-element array of this antenna has been formed, and wide-band radiation properties of the array are reported.

1. INTRODUCTION

Wide-band solution in antenna design is becoming more challenging as the number of bands used in the world is increasing. For base station antenna design, it becomes more complex as manufacturers tend to prefer one antenna solution for worldwide products. The antenna is one of the biggest parts of the base station head unit. The most challenging case is the lower part of operating bands of the E-UTRA system, as lower frequency means larger antenna. According to 3GPP E-UTRA operating bands standard [1], lower part of frequencies, which are partially implemented and going to implement worldwide in the future, ranges from 698 MHz to 960 MHz. For an antenna designer, the main challenge is to find an antenna solution which will cover low-band frequencies that satisfies typical radiation properties of a directional base station antenna.

Widening bandwidth of a patch antenna has been done in many ways. Typically parasitic patch and L-probe feeding have become the popular techniques for wide-band solutions. An analysis of L-probe-fed technique is described in [2, 3]. A dual-band dual-fed L-probe patch antenna has been reported in [4]. In those papers mainly the L-shaped probe structure and its working principle have been described in detail. Bandwidth increase by parasitic patch has been reported in [5, 6]. Capacitive fed technique, which is used to increase GPS antenna bandwidth, has been described in [7]. L-probe fed circular patch antenna with 30% bandwidth ($VSWR \leq 2$) is reported in [8] and has conical shape radiation patterns. Circular patch antenna mode excitation, substrate height, dielectric properties and ground plane effects have been studied in [9]. Some articles [10–13] have reported different patch shapes and patch alteration methods to increase bandwidth. A U-shaped slot wide-band patch antenna with 47% bandwidth ($VSWR \leq 2$) and asymmetric radiation patterns in two planes is presented in [10]. However, wide-band radiation properties have not been reported in that article. Multiple U-slots and V-slots for multiple narrow band resonances with L-probe fed antenna are reported in [11]. An L-probe fed H-shaped patch antenna with 22.63% bandwidth at 10 dB return loss is presented in [12]. A direct fed wide-band E-shaped patch antenna design with 30% bandwidth at 10 dB return loss and analysis of multiband E-shaped direct fed patch antenna have been discussed in [13, 14]. The ground plane size effect on antenna properties

Received 20 October 2015, Accepted 11 December 2015, Scheduled 22 December 2015

* Corresponding author: Muhammad Nazrul Islam (nazrul.islam@esju.com).

¹ Esju Oy, Oulu, Finland. ² Center for Wireless Communication at the University of Oulu, Finland.

such as radiation patterns and input impedance both of circular and rectangular patches are studied in [15, 16]. An array of four elements of wide-band L-probe is reported in [17]. This antenna array reported bandwidth coverage is 22.2% ($VSWR < 1.5$). As we have discovered, increasing bandwidth by combining different patch shapes such as circular and elliptical patches and covering 45% bandwidth by such an antenna array has not been found.

In this paper, a very wide-band patch antenna design by the combination of a main patch shape and parasitic patch shape in L-probe fed technique has been achieved. This unique patch combination with L-probe excites wide-band resonances. A two-element array made of this antenna has been built, and its wide-band symmetric response over the whole bandwidth has achieved. CST Microwave Studio simulation tool has been used to calculate antenna properties. Calculated results are validated by building the model and measuring antenna properties.

2. DESIGN PROCEDURE

2.1. Design of a Wide-Band L-Probe Fed Patch Antenna by Main and Parasitic Patch Shapes

Design focus was to design an antenna suitable for all E-UTRA low bands (699 MHz to 960 MHz). After many trials, an adequate broad band L-probe fed patch antenna structure was found. This antenna has one main patch and two parasitic patches. Parasitic patches are on a PCB's top and bottom layers. Design goal was to achieve broad band response by patch shape, patch dimensions and patch combinations. Patch shape and dimension optimizations were done by trial and error as trial and error process is a common practice in most patch antenna design. An optimized L-probe fed patch antenna with 100 ohm input impedance was found.

This optimized L-probe fed patch antenna has a circular shape main patch close to L-probe fed and two elliptical shape patches on a PCB's top and bottom layers. An elevated single element antenna structure and its different parts are shown in Fig. 1. The circular patch is a 1 mm thick brass metal plate, and PCB patches are 30 μm thick two-layered elliptical shape copper on a 1.5 mm thick FR4 substrate. The spacing between L-probe and main patch and spacing between main patch and PCB were chosen by iteration. In this optimization process, manufacturing compatibility has been factored in. An optimized combination of patches and their shapes provide multiple resonances and give a wide-band solution. For the right spacing between patches and L-probe, plastic screws support has been used. These screws also assist to adjust the height properly. All the spacing is shown in Fig. 1. L-probe was supported with foam to the ground plate. This foam has approximate air dielectric properties. The detailed dimensions of the circular metal patch and PCB elliptical patches are shown in Fig. 2.

L-probe feeding structure and its relative position from circular patch center are shown in Fig. 3.

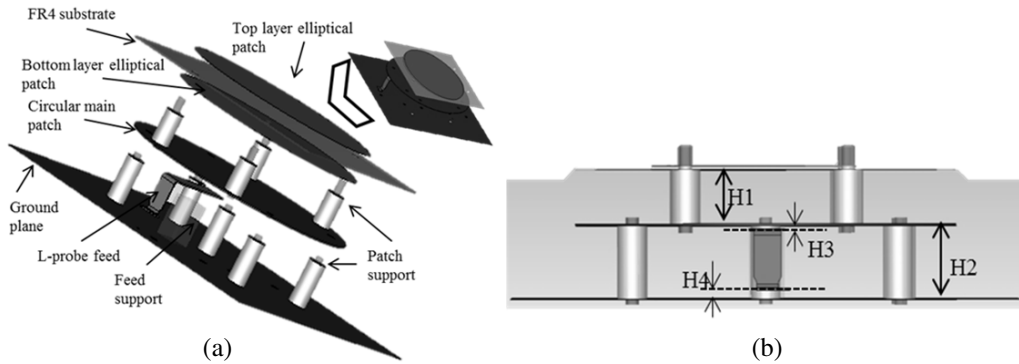


Figure 1. (a) Elevated single element patch 3D shape. (b) Side view single element, spacing between circular patch and PCB, $H1 = 25$ mm, spacing between circular patch and ground, $H2 = 33.6$ mm, spacing between circular patch and L-probe fed $H3 = 1.2$ mm, spacing between L-probe fed bottom and ground, $H4 = 4$ mm.

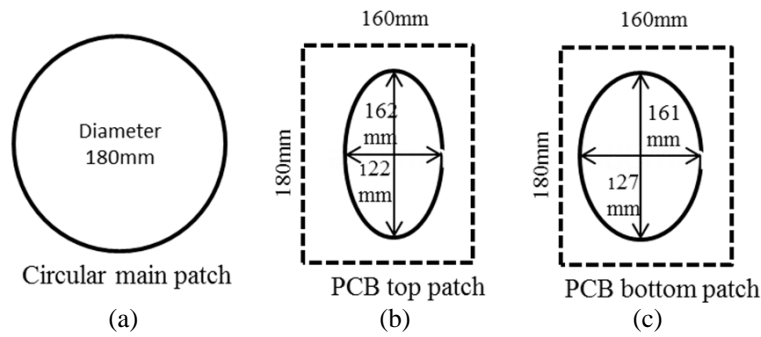


Figure 2. (a) Circular main patch. (b) Elliptical patch on PCB top. (c) Elliptical patch on PCB bottom.

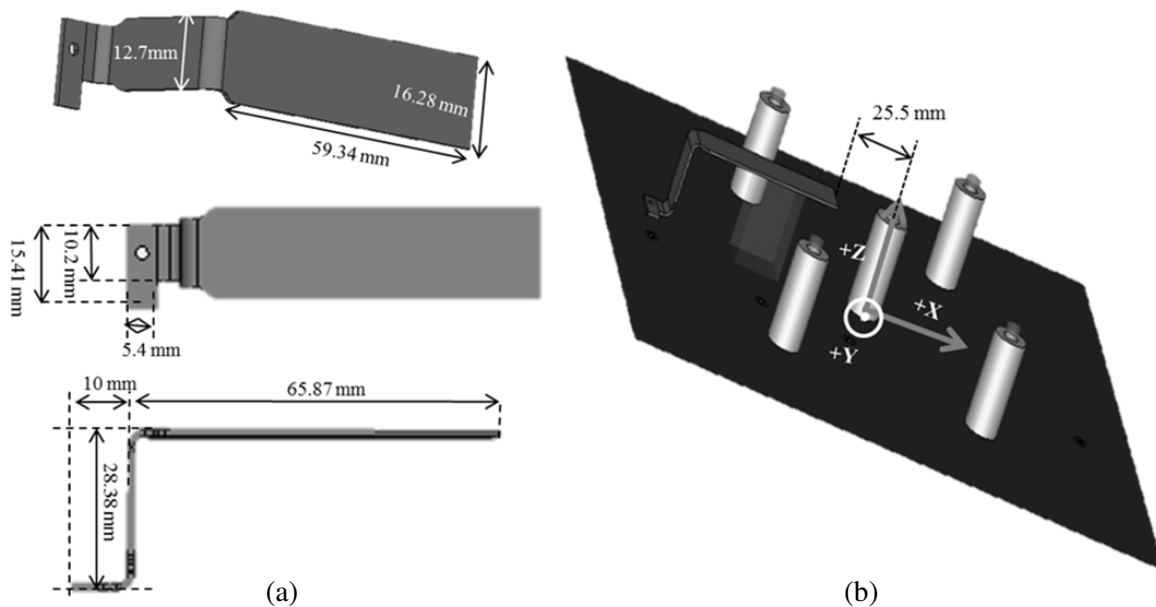


Figure 3. (a) L-probe fed structure. (b) Circular patch center and L-probe edge spacing.

L-probe fed top part is aligned to the circular patch diagonal. According to this figure, it is clear that this antenna has been designed for X direction polarization. End of the L-probe bottom part has been connected to the antenna array feeding network in a two-element array design. 1 mm thick copper metal is used in this feed line design.

To show optimization process, six simulation cases described in Table 1 are reported here. A comparative bandwidth coverage simulation result with one element has been shown in Fig. 4. Different patch shapes have been studied. This is an example result for optimizing patch shape and patch combinations. There have been many other patch shapes and dimensions tried out to achieve similar band coverage within the same volume without success. To avoid data redundancy, those are not reported. From these simulation results, it is evident that optimized patch shapes and their combination meet the broad band return loss. In this comparative simulation, all other parameters of the antenna were kept constant. For example, in the main patch square case only main patch is changed with square shape, and all other parts of the antenna are the same as the optimized one. It is clear that optimum patch shapes and their combination provide wide-band (690 MHz–960 MHz) coverage. Fig. 5 shows comparison of return loss between optimized patch combination antenna and only main circular patch antenna simulation results. This shows multiple resonances creation and widening bandwidth by designed patch combinations.

Table 1. Optimization simulation cases.

Simulation cases	Main patch	PCB bottom patch	PCB top patch
Optimized antenna Case-1	Circular: diameter 180 mm	Elliptical: major axis 161 mm, minor axis 127 mm	Elliptical: major axis 162 mm, minor axis 122 mm
Case2-main patch square	Square patch: side 180mm	Same as optimized	Same as optimized
Case3-PCB bottom patch circular	Same as optimized	Circular: diameter 161 mm	Same as optimized
Case4-PCB top patch circular	Same as optimized	Same as optimized	Circular-diameter 162 mm
Case5-PCB bottom patch square	Same as optimized	Square patch: side 161 mm	Same as optimized
Case6-PCB top patch square	Same as optimized	Same as optimized	Square patch: side162 mm

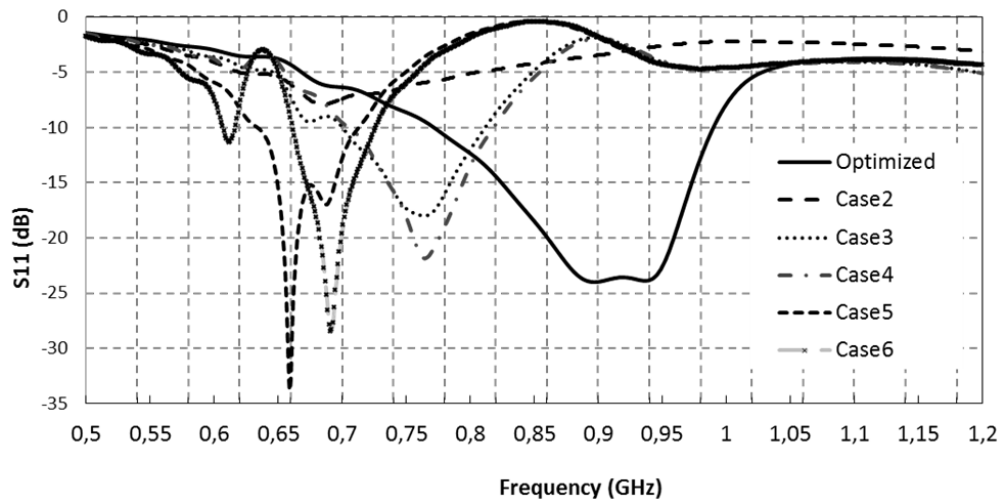


Figure 4. Simulated reflection coefficients for different patch shape combinations defined in Table 1.

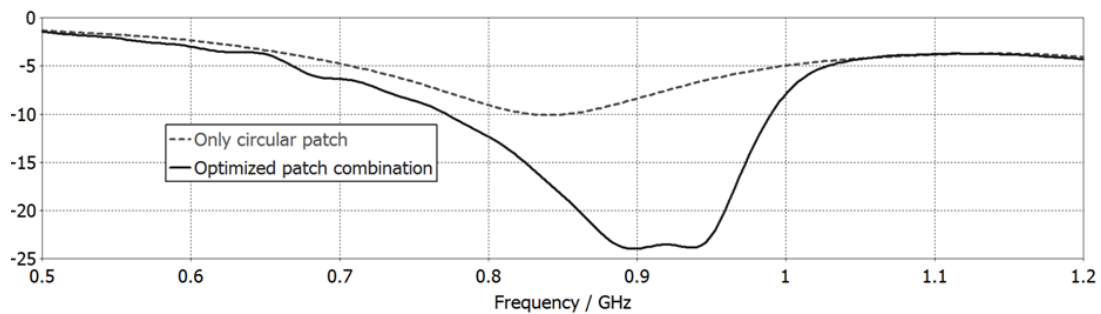


Figure 5. Simulated reflection coefficients for only circular patch and optimized patch combination.

2.2. Two-Element Array

In the two-element array design, 0.7λ (at 830 MHz) spacing between the antennas is used. After getting a suitable antenna element and right spacing for the two-element array, one corporate feeding network was designed. Each end of the feeding network is connected to an L-probe fed end. As each element has 100 ohm input impedance, a separate impedance transformer was not needed in its fed network design. In this two-element combiner, T-junction natural output comes as 50 ohm input impedance. Fig. 6 shows major dimension of the feeding network. The gap between ground and 100 ohm strip line is 4 mm. In 50 ohm strip line, this gap is 2 mm. In this fed lines design, strip line turn truncation and T-junction tapering has been optimized for impedance matching and less loss. This T-junction combiner and transmission line can be designed with different ground spacings and strip line widths.

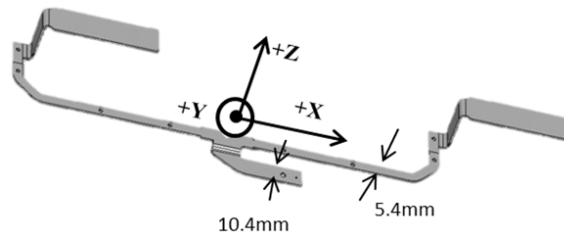


Figure 6. Fed combiner for two-element array and L-probe fed structure.

A two-element antenna array has been manufactured to examine its array performance for wide frequency range. The manufactured antenna array is shown in Fig. 7. This array is built on 240 mm width and 480 mm long ground plane. All plastic screws gaps are adjusted to the height of the simulation model. The screws on the trace line make this structure quite stable on the ground plane. Spacings between traces and ground plane are maintained by small plastic bushing, which has less effect on transmission line properties.

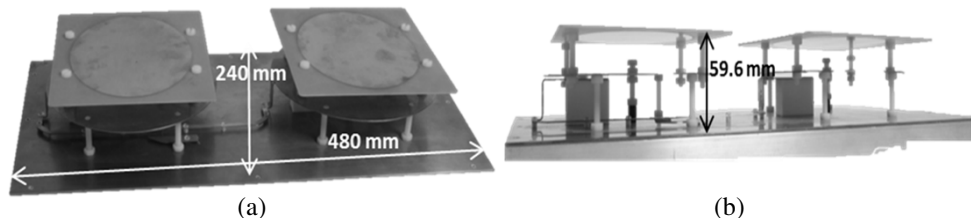


Figure 7. (a) Two-element array structure. (b) Patch and fed line fixing mechanics.

3. PERFORMANCE

The manufactured antenna array has been measured and compared with the calculated results. Fig. 8 shows the measured and simulated reflection coefficient plots. Simulation results of the array show better broad band performance than single element simulation results. This comes from an array form of two antenna elements with feeding network. Antenna array measurement and simulation match quite adequately, and the measurement shows that this array has more than 45%, -10 dB matched band width. Measurement is slightly better than the simulation result, and this could come from human error in accuracy of different parts fixing. This array has eight screws for patches and nine screws on feeding network. Making exact elliptical shape on PCB has also design challenge. Measured results also prove that the designed array has an easy option to optimize its return loss. This manufactured array has more than 12 dB return loss in required bandwidth. Measurement has been taken at the array feed point where one SMA connector was soldered to the array base ground, and the SMA center pin was soldered at the array feed point. In this case, no cable loss is counted.

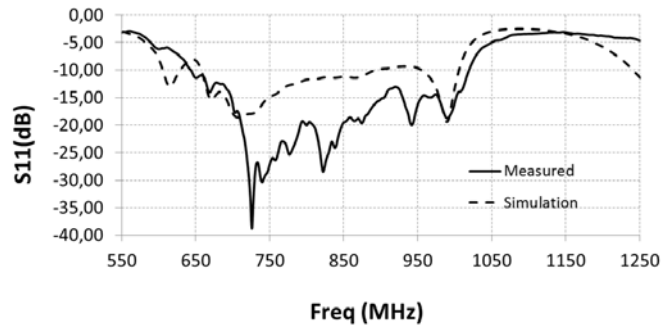


Figure 8. Measured and simulated reflection coefficients for the two-element array.

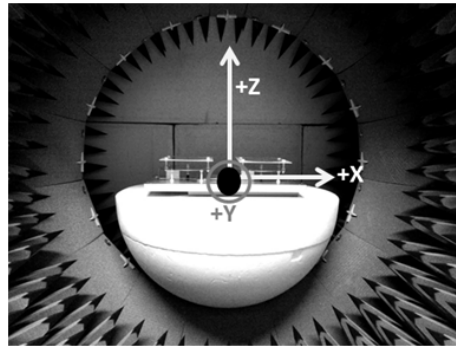


Figure 9. Antenna array placement in the measurement chamber.

Antenna array radiation properties have been measured in the near-field measurement system (SatimoStarLab) at the Department of Communications Engineering, University of Oulu. This antenna ground plane (48 cm) is slightly larger than the maximum guaranteed size (40 cm) of the DUT in which particular chamber and measurement accuracy below 800 MHz is not recommended. The chamber was calibrated from 700 MHz. Despite this limitation, the antenna array has been measured from 700 MHz to 1000 MHz. This measurement gives us measured and calculated values for comparative validation particularly above 800 MHz.

The near-field antenna measurement chamber's coordinate system and the antenna placement in the chamber are shown in Fig. 9. From this coordinate system and antenna placement in it, we can find elevation (XZ plane or E plane) and azimuth (YZ plane or H plane) antenna patterns. Fig. 10 presents both simulated and measured total radiation efficiencies. From efficiency plot, it is evident that this antenna array radiates efficiently at its resonance frequencies. There is a small discrepancy between measurement and simulation, and it is more prominent below 800 MHz. Part of this comes from inaccurate chamber below 800 MHz.

The antenna array maximum gains, both from measurement and simulation are plotted in Fig. 11. The simulation and measurement correlate well. The max gain varies from 9 dBi to 11.49 dBi within the whole bandwidth. Lower frequencies have slightly lower max gain than the max gain at the frequencies of 850 MHz to 960 MHz.

Antenna radiation patterns, both for co- and cross-polarized components in E plane (XZ plane) and H plane cuts (YZ plane) at different frequencies are shown in Fig. 12. Radiation patterns show consistency over all frequencies and low cross polarized component in vertical plane. Main lobe small tilt is observed, and this comes from small phase change between the two elements for its feeding point asymmetry. Front to back ratio is 15 dB in the most parts of the band. Table 2 gives a measured half power beam width at different frequencies both in E and H plan cuts. The wider half power beam width in H plane cut and less side lobes in E plane cut are observed. These are desirable requirement for direction antenna array.

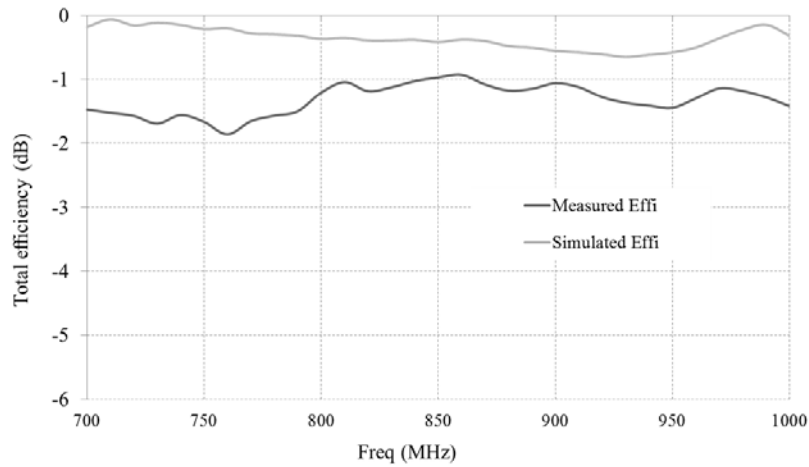


Figure 10. Measured and simulated total efficiency for antenna array.

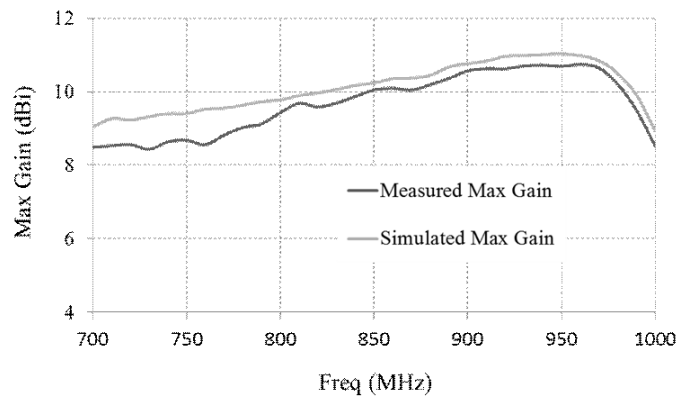


Figure 11. Measured and simulated maximum gains for the two-element array.

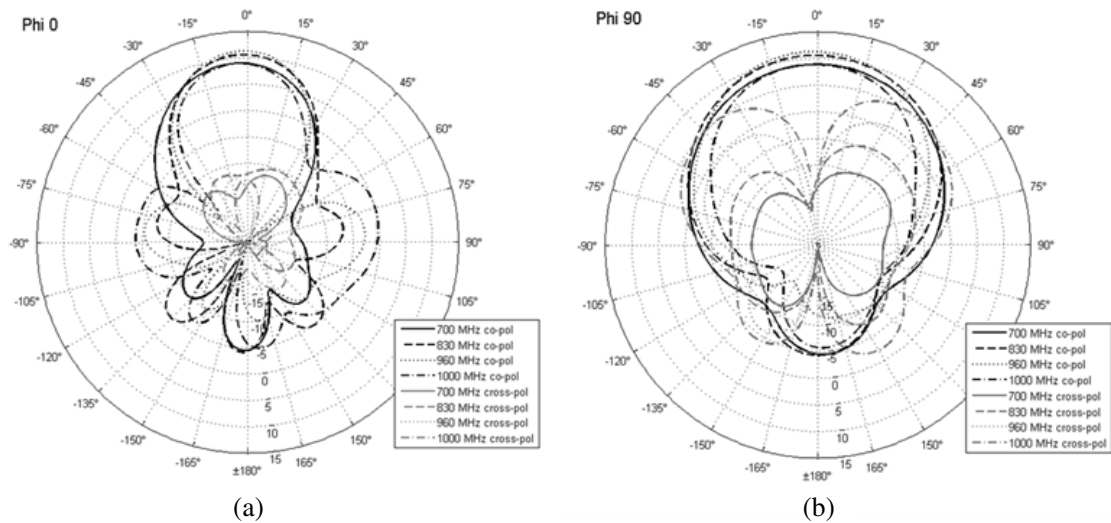


Figure 12. (a) Measured radiation pattern at array *E*-plane cut, (b) radiation pattern at array *H*-plane cut.

Table 2. Half power beam width (HPBW) in E and H plane of the array.

Frequency (MHz)	HPBW E -plane	HPBW in H -plane
700	51	96
830	48	98
960	40	93
1000	39	120

4. CONCLUSION

A unique wide-band patch antenna design and an array of two elements of this antenna is found and validated by proto build and measurement. A consistent array performance across the band shows that this design concept is a good candidate for wide-band high gain patch antenna array design. From this calculation and measurement it is found that by choosing appropriate patch shapes and their combination, it is possible to get a very wide-band response in L-probe feed technique. Such relative bandwidth (45%) patch antenna array has not been found before, as far as we know. Further tuning of reflection coefficient and optimization over the desire frequency band can be done in feeding network, patches and height. Reducing overall height of the antenna and making this design as low profile design could be a future design task. In addition to this, a dual-polarized wide-band solution can be tried out for future study.

ACKNOWLEDGMENT

The first author, Muhammad Nazrul Islam, would like to thank Oulu University workshop and Kai Schröder from Esju Oy.

REFERENCES

1. E-UTRA operating bands, 3GPP TS 36.101 Var 10.10.0 [Online]. Available: http://www.3gpp.org/ftp/Specs/2013-03/Rel-10/36_series/.
2. Guo, Y. X., K. M. Luk, and K.-F. Lee, "L-Probe fed thick-substrate patch antenna mounted on a finite ground plane," *IEEE Trans. Antennas and Propagation*, Vol. 21, No. 21, 1955–1963, Aug. 2003.
3. Guo, Y.-X., C.-L. Mak, and K.-M. Luk, "Analysis and design of L-probe proximity fed patch antenna," *IEEE Trans. Antennas and Propagation*, Vol. 49, No. 2, 145–149, Feb. 2003.
4. Li, P., K. M. Luk, and K. L. Lau, "A dual-feed dual-band L-probe patch antenna," *IEEE Trans. Antennas and Propagation*, Vol. 53, No. 7, 2321–2323, Jul. 2005.
5. Lee, R. Q. and J. Bobinchak, "Characteristics of a two-layer electromagnetically coupled rectangular patch antenna," *Electronics Letters*, Vol. 23, No. 20, 24, Sep. 1987.
6. Wood, C., "Improved bandwidth of microstrip antennas using parasitic elements," *IEE Proc.*, Vol. 127, Pt. H, No. 4, Aug. 1980.
7. Islam, M. N., S. I. Karhu, and E. T. Salonen, "GPS and GSM antenna with a capacitive feed for a personal navigator device," *Wireless Information Technology and Systems (ICWITS)*, 2010.
8. Guo, Y. X., K. M. M.W. Chia, Z. N. Chen, and K.-M. Luk, "Wide-band L-probe fed circular patch antenna for conical-pattern radiation," *IEEE Trans. Antennas and Propagation*, Vol. 52, No. 4, 1115–1116, Apr. 2004.
9. Kishk, A. A. and L. Shafai, "The effect of various parameters of circular microstrip antennas on their radiation efficiency and mode excitation," *IEEE Trans. Antennas and Propagation*, Vol. 34, 1310–1312, Aug. 1995.

10. Huynh, T. and K. F. Lee, "Single-layer single-patch wideband microstrip antenna," *Electronics Letters*, Vol. 31, No. 16, 1310–1312, Aug. 1995.
11. Salamat, C. D., M. Haneishi, and Y. Kimura, "L-probe fed multiband microstrip antennas with slots," *Proceeding of Asia-Pacific Microwave Conference*, 2006.
12. Ali, M. T., N. Nordin, I. Pasya, and M. N. Md Tan, "H-shaped microstrip patch antenna using L-probe fed for wide-band application," *6th European Conference on Antenna and Propagation*, Mar. 26–30, 2012.
13. Yang, F., X.-X. Zhang, X. Ye, and Y. Rahmat-Samii, "Wide-band E-shaped patch antennas for wireless communications," *IEEE Trans. Antennas and Propagation*, Vol. 49, No. 7, 1094–1100, Jul. 2001.
14. Jin, N. and Y. Rahmat-Samii, "Parallel particle swarm optimization and finite-difference time-domain (PSO/FDTD) algorithm for multiband and wide-band patch antenna designs," *IEEE Trans. Antennas and Propagation*, Vol. 53, No. 11, 3459–3468, Nov. 2005.
15. Bhattacharyya, A. K., "Effects of finite ground plane on the radiation characteristics of a circular patch antenna," *IEEE Trans. Antennas and Propagation*, Vol. 38, 152–159, Feb. 1990.
16. Lier, E. and K. R. Jakobsen, "Rectangular microstrip patch antennas with infinite and finite ground plane dimensions," *IEEE Trans. Antennas and Propagation*, Vol. 31, No. 7, 978–984, Nov. 1983.
17. Lo, W. K., K. M. Shum, C. H. Chan, and K. M. Luk, "Wide-band L-probe fed base-station antenna array for PCS communication," *Antennas and Propagation Society International Symposium*, Vol. 2, 200–203, Nov. 1983.